Lesson 41

The Windowed Fourier Transform

41.1 Limitations of standard Fourier analysis

Current research is to a large extent motivated by industrial applications of mathematical analysis and signal processing. Seismic exploration, the analysis and synthesis of sound, medical imaging, and the digital telephone are a few of the applications that come to mind. In all cases, one wishes to extract from the signal the pertinent information as discrete numerical values. This set of digital information must be rich enough to characterize the signal, but it should be no larger than necessary for the task at hand. If, for example, it is a question of speech and the digital telephone, one wants enough numerical information at the receiver to reconstruct a recognizable voice, but economy dictates the need to minimize the amount of information that must be transmitted.

Fourier analysis is the oldest of the various techniques avaliable for signal analysis and synthesis. Since the invention of the fast Fourier transform (FFT), it has become an efficient tool, particularly for analyzing sufficiently smooth periodic signals (Lesson 9). In these cases, the Fourier coefficients c_n decrease rapidly as $|n| \to +\infty$, and relatively few numerical coefficients are needed to reconstruct the signal for most practical purposes. Unfortunately, as soon as the signal becomes irregular, like, for example, a transient, the number of coefficients necessary to reconstruct the signal (and hence the amount of data that must either be stored or transmitted) becomes large and often economically impractical.

Before the advent of the FFT, Fourier analysis was mainly a theoretical tool—indeed, one of the most important and pervasive. This quickly changed with the arrival of the FFT and efficient digital computing, and these twin techniques have had widespread applications in the last third of the twentieth century. Nevertheless, even with the FFT and modern computing, Fourier analysis does not provide a satisfactory analysis for all kinds of signals. Although the Fourier transform $\hat{f}$ contains all of the information about f, much of this information in "hidden." For example, none of the temporal aspects of f are revealed by $\widehat{f}$. If f is a finite signal, the spectrum does not indicate the beginning and the end of the signal, and if there is a singularity, the time of occurrence is hidden throughout $\widehat{f}$.

Faced with these kinds of issues, one would like to have an analytic tool that provides information both in time and in frequency. The model that is often cited is musical notation: the horizontal position of a note (its "start time," its duration, and its frequency are all represented.

There is another problem that has surely not escaped the reader's notice: To compute the spectrum $\widehat{f}(\lambda)$ it is necessary to know $f(t)$ for all real values of t. This is impossible in the case of analysis in "real time" where the signal must be processed as it arrives. One cannot know the spectrum, even approximately, of a signal when one knows nothing of its future; the interesting information may be yet to arrive. We should not despair, however; the previous eleven chapters retain their value today both theoretically and numerically in spite of the cited problems. These technical constraints simply motivate us to refine existing tools and to develop new ones.

41.2 Opening windows

One of the first ideas was to truncate the signal and to analyze only what happens on a finite interval $[-A, A]$. One is forced to do this when making numerical computations. Mathematically, this amounts to multiplying the signal $f(t)$ by a characteristic function $\chi_{[-A,A]} = r_A$ (or a translate) and taking the Fourier transform of the product. The result is

$$\widehat{g}(\lambda) = \widehat{r_A \cdot f}(\lambda) = \left(\frac{\sin 2\pi A\lambda}{\pi\lambda}\right) * \widehat{f}(\lambda) = (s_A * \widehat{f})(\lambda).$$

Thus truncating the signal results in convolving its spectrum with the cardinal sine (Figure 41.1).

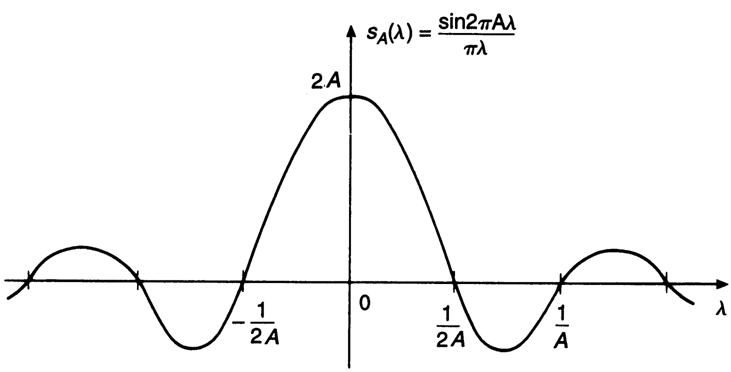

FIGURE 41.1. The cardinal sine.

The approximation of $\widehat{f}$ by $\widehat{g}$ becomes better as A increases, that is, as s_A better approximates the Dirac impulse. Unfortunately, the computations for this process quickly become very voluminous. The cardinal sine decays slowly and has important lobes near the origin. To avoid these problems, one replaces $\chi_{[-A,A]}$ with a more regular function. These functions are all called windows, and they are concentrated around the origin.

EXAMPLES:

(a) *Triangular window* (Figure 41.2)

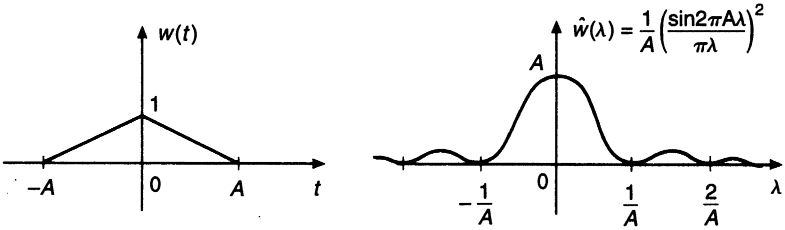

FIGURE 41.2. Triangular window in time and frequency.

(b) *Hamming and Hanning windows* (Figure 41.3)

These are of the form $\omega(t) = [\alpha + (1-\alpha)\cos(2\pi t/A)]r(t)$. For $\alpha = 0.54$ we have Hamming's window and for $\alpha = 0.50$ Hanning's window. These coefficients have been computed to minimize certain criteria (see [Kun84]).

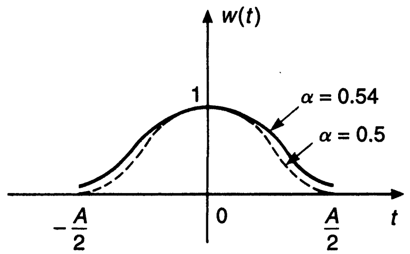

FIGURE 41.3. Hamming and Hanning windows.

(c) *Gaussian window* $\omega(t) = Ae^{-\alpha t^2}$ $(\alpha, A > 0)$ (Figure 41.4)

These windows are used in practice, and they significantly improve the computation of the spectrum.

One is led naturally to slide this window along the graph of the function and thereby analyze the whole function. One then obtains a family of coefficients depending on two real variables λ and b given by

$$W_f(\lambda, b) = \int_{-\infty}^{+\infty} f(t)\overline{w}(t-b)e^{-2i\pi\lambda t}\,dt. \tag{41.1}$$

$W_f(\lambda, b)$ replaces $\widehat{f}(\lambda)$. The mapping $f \mapsto W_f$ is called the *sliding window Fourier transform* or simply the *windowed Fourier transform*.

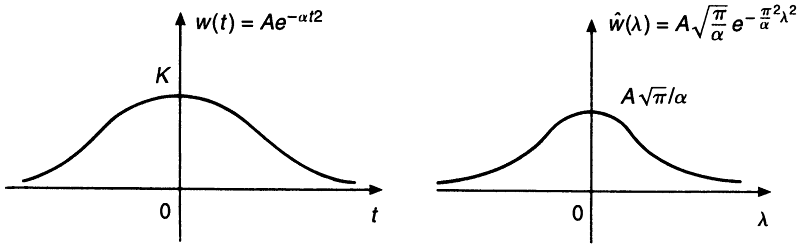

FIGURE 41.4. Gaussian window in time and frequency.

The parameter λ plays the role of a frequency, localized around the abscissa b of the temporal signal. $W_f(\lambda, b)$ thus provides an indication of how the signal behaves at time $t = b$ for the frequency λ. We use the function $\overline{\omega}$ rather than ω in (41.1) for reasons of convenience and because we wish to allow complex-valued windows. Thus, W_f becomes a scalar product in L^2:

$$\begin{aligned} W_f(\lambda, b) &= (f, w_{\lambda b}), \\ w_{\lambda b}(t) &= w(t-b)e^{2i\pi\lambda t}. \end{aligned} \tag{41.2}$$

41.3 Dennis Gabor's formulas

Intuitively, one might expect that knowing $W_f(\lambda, b)$ for all values of λ and b completely determines the signal f. One could even conjecture that the information contained in $W_f(\lambda, b)$ is redundant, since we have replaced a one-parameter family $\widehat{f}$ with a two-parameter family. We will see below that these speculations are well founded.

In his 1946 paper [Gab46], Dennis Gabor used a window that was essentially the Gaussian $w(t) = \pi^{-1/4}e^{-t^2/2}$. Such a function has the advantage of approximating a square window while avoiding the disadvantage of introducing abrupt discontinuities. One of Gabor's important contributions was to show that $W_f(\lambda, b)$ can be inverted to recover f.

41.3.1 Theorem *Suppose that $w \in L^1 \cap L^2$ is a window such that $|\widehat{w}|$ is even and $\|w\|_2 = 1$. Write*

$$w_{\lambda b}(t) = w(t-b)e^{2i\pi\lambda t}, \quad \lambda, b \in \mathbb{R}.$$

For all signals $f \in L^2$ we define the coefficients

$$W_f(\lambda, b) = \int_{-\infty}^{+\infty} f(t)\overline{w}_{\lambda b}(t)\,dt.$$

Under these conditions, we have the following two results:

(a) *Conservation of energy:*

$$\iint_{\mathbb{R}^2} |W_f(\lambda, b)|^2 \, d\lambda \, db = \int_{-\infty}^{+\infty} |f(t)|^2 \, dt. \tag{41.3}$$

(b) *Reconstruction formula:*

$$f(x) = \iint_{\mathbb{R}^2} W_f(\lambda, b) w_{\lambda b}(x) \, d\lambda \, db \tag{41.4}$$

in the sense that if

$$g_A(x) = \iint_{\substack{|\lambda| \le A \\ b \in \mathbb{R}}} W_f(\lambda, b) w_{\lambda b}(x) \, d\lambda \, db,$$

then $g_A \to f$ *in* L^2 *as* $A \to +\infty$.

Proof. We first give another expression for $W_f(\lambda, b)$:

$$W_f(\lambda, b) = \int_{-\infty}^{+\infty} f(t) \overline{w}_{\lambda b}(t) \, dt = \int_{-\infty}^{+\infty} \widehat{f}(\xi) \overline{\widehat{w}}_{\lambda b}(\xi) \, d\xi.$$

Since

$$\widehat{w}_{\lambda b}(\xi) = e^{-2i\pi(\xi - \lambda)b} \widehat{w}(\xi - \lambda), \tag{41.5}$$

this becomes

$$W_f(\lambda, b) = e^{-2i\pi\lambda b} \int_{-\infty}^{+\infty} \widehat{f}(\xi) \overline{\widehat{w}}(\xi - \lambda) e^{2i\pi\xi b} \, d\xi,$$

so

$$W_f(\lambda, b) = e^{-2i\pi\lambda b} \overline{\mathscr{F}}_{\xi} [\widehat{f}(\xi) \overline{\widehat{w}}(\xi - \lambda)](b). \tag{41.6}$$

The function of ξ in brackets is in L^1, since it is the product of two functions in L^2. It is also in L^2 because, w being in L^1, $\widehat{w}$ is bounded. Thus we have

$$\begin{aligned}
\iint_{\mathbb{R}^2} |W_f(\lambda, b)|^2 \, d\lambda \, db &= \int_{-\infty}^{+\infty} \left(\int_{-\infty}^{+\infty} |\overline{\mathscr{F}}_{\xi} [\widehat{f}(\xi) \overline{\widehat{w}}(\xi - \lambda)](b)|^2 \, db \right) d\lambda \\
&= \int_{-\infty}^{+\infty} \left(\int_{-\infty}^{+\infty} |\widehat{f}(\xi) \overline{\widehat{w}}(\xi - \lambda)|^2 \, d\xi \right) d\lambda \quad \text{(Parseval)} \\
&= \int_{-\infty}^{+\infty} \left(|\widehat{f}(\xi)|^2 \int_{-\infty}^{+\infty} |\widehat{w}(\xi - \lambda)|^2 \, d,\lambda \right) d\xi \\
&= \|f\|_2^2 \|\widehat{w}\|_2^2 = \|f\|_2^2.
\end{aligned}$$

This establishes (a).

To prove (b), we first show that g_A is well-defined for all $A > 0$ by showing that $(\lambda, b) \mapsto W_f(\lambda, b) w_{\lambda b}(x)$ is integrable on the strip $[-A, A] \times \mathbb{R}$. Let

$$J_A(x) = \int_{-A}^{A} \left(\int_{-\infty}^{+\infty} |\overline{\mathscr{F}}_{\xi}[\widehat{f}(\xi)\overline{\widehat{w}}(\xi - \lambda)](b)|\, |w(x-b)|\, db \right) d\lambda.$$

By Schwarz's inequality and Parseval's relation, we have (Theorem 22.1.4)

$$\begin{aligned} J_A(x) &\le \int_{-A}^{A} \|\overline{\mathscr{F}}_{\xi}[\widehat{f}(\xi)\overline{\widehat{w}}(\xi - \lambda)](b)\|_2 \|w\|_2 \, d\lambda \\ &= \int_{-A}^{A} \|\widehat{f}(\xi)\overline{\widehat{w}}(\xi - \lambda)\|_2 \, d\lambda. \end{aligned}$$

The function $h(\lambda)$ under the last integral sign satisfies

$$h^2(\lambda) = \int_{-\infty}^{+\infty} |\widehat{f}(\xi)|^2 |\widehat{w}(\xi - \lambda)|^2 \, d\xi = (|\widehat{f}|^2 * |\widehat{w}|^2)(\lambda).$$

Since $L^1 * L^1 \subset L^1$, it follows that $|h|^2 \in L^1$ and hence that $h \in L^2$. Finally,

$$J_A(x) \le \int_{-A}^{A} h(\lambda)\, d\lambda \le \sqrt{2A}\|h\|_2 < +\infty$$

for all $x \in \mathbb{R}$ and $A > 0$. Integrability allows us to choose the order of integration in the definition of g_A, so in view of (41.6), we have

$$g_A(x) = \int_{-A}^{A} g(\lambda)\, d\lambda$$

with

$$g(\lambda) = \int_{-\infty}^{+\infty} \overline{\mathscr{F}}_{\xi}[\widehat{f}(\xi)\overline{\widehat{w}}(\xi - \lambda)](b) w(x-b) e^{2i\pi\lambda(x-b)}\, db,$$

which by Proposition 22.1.5 is

$$g(\lambda) = \int_{-\infty}^{+\infty} \widehat{f}(\xi)\overline{\widehat{w}}(\xi - \lambda) \overline{\mathscr{F}}_{b}[w(x-b)e^{2i\pi\lambda(x-b)}](\xi)\, d\xi.$$

After computing the Fourier transform $\overline{\mathscr{F}}_{b}[w(x-b)e^{2i\pi\lambda(x-b)}]$, we see that

$$g(\lambda) = \int_{-\infty}^{+\infty} \widehat{f}(\xi)\overline{\widehat{w}}(\xi - \lambda)\widehat{w}(\xi - \lambda) e^{2i\pi\xi x}\, d\xi,$$

so

$$g_A(x) = \int_{-A}^{A} \left(\int_{-\infty}^{+\infty} \widehat{f}(\xi) |\widehat{w}(\xi - \lambda)|^2 e^{2i\pi\xi x}\, d\xi \right) d\lambda. \tag{41.7}$$

The next step is to verify that the function of (λ, ξ) under the double integral (41.7) is integrable on $[-A, A] \times \mathbb{R}$. Since $|\widehat{w}|$ is even,

$$\int_{-A}^{A} \left(\int_{-\infty}^{+\infty} |\widehat{f}(\xi)| |\widehat{w}(\xi - \lambda)|^2 \, d\xi \right) d\lambda = \int_{-A}^{A} (|\widehat{f}| * |\widehat{w}|^2)(\lambda) \, d\lambda.$$

Since $|\widehat{f}| \in L^2$ and $|\widehat{w}|^2 \in L^1$, it follows (Proposition 20.3.2) that $h = |\widehat{f}| * |\widehat{w}|^2 \in L^2(\mathbb{R})$ and hence that $h \in L^1[-A, A]$. Thus the integral is well-defined, and we can interchange the order of integration in (41.7):

$$g_A(x) = \int_{-\infty}^{+\infty} \widehat{f}(\xi) e^{2i\pi\xi x} \left(\int_{-A}^{A} |\widehat{w}(\xi - \lambda)|^2 \, d\lambda \right) d\xi.$$

Denote the second integral by $\varphi_A(\xi)$. Then $0 \le \varphi_A(\xi) \le 1$, since $\|\widehat{w}\|_2 = 1$. Since φ_A is bounded, $\widehat{f}\varphi_A$ is in L^2 and $g_A = \overline{\mathscr{F}}(\widehat{f} \cdot \varphi_A)$. The last step is to show that g_A tends to f in L^2 as $A \to +\infty$. For this we evaluate the norm of the difference:

$$\|f - \overline{\mathscr{F}}(\widehat{f} \cdot \varphi_A)\|_2^2 = \|\overline{\mathscr{F}}[(1 - \varphi_A)\widehat{f}\,]\|_2^2 = \|(1 - \varphi_A)\widehat{f}\,\|_2^2 = \varepsilon(A).$$

We estimate the integral

$$\varepsilon(A) = \int_{-\infty}^{+\infty} [1 - \varphi_A(\xi)]^2 |\widehat{f}(\xi)|^2 \, d\xi \tag{41.8}$$

in two parts. If $|\xi| \le A/2$, then

$$1 - \varphi_A(\xi) = \int_{|\lambda| \ge A} |\widehat{w}(\xi - \lambda)|^2 \, d\lambda = \int_{-\infty}^{\xi - A} |\widehat{w}(y)|^2 \, dy + \int_{\xi + A}^{+\infty} |\widehat{w}(y)|^2 \, dy,$$

so

$$0 \le 1 - \varphi_A(\xi) \le \int_{-\infty}^{-\frac{A}{2}} |\widehat{w}(y)|^2 \, dy + \int_{\frac{A}{2}}^{+\infty} |\widehat{w}(y)|^2 \, dy = \varepsilon_1(A),$$

which tends to 0 as $A \to +\infty$. As a consequence,

$$\int_{-\frac{A}{2}}^{\frac{A}{2}} [1 - \varphi_A(\xi)]^2 |\widehat{f}(\xi)|^2 \, d\xi \le \varepsilon_1^2(A) \|f\|_2^2.$$

If $|\xi| \ge A/2$, then

$$\int_{|\xi| \ge \frac{A}{2}} [1 - \varphi_A(\xi)]^2 |\widehat{f}(\xi)|^2 \, d\xi \le \int_{|\xi| \ge \frac{A}{2}} |\widehat{f}(\xi)|^2 \, d\xi,$$

which also tends to 0 as $A \to +\infty$. These two estimates show that $\varepsilon(A)$ (41.8) tends to 0 as A tends to infinity, and this proves (b). □

This result shows that for the windowed Fourier transform in L^2 we have formulas analogous to those for the ordinary Fourier transform in L^2: conservation of energy (Parseval's formula) and an inversion formula. There is a nice harmony in these formulas; this will also appear in the theory of wavelets.

In practice, one generally uses a function w that is well localized around the origin $t = 0$, for example, a Gaussian. The function $w_{\lambda b}$ is then localized around the point $t = b$, while $\widehat{w}_{\lambda b}$, given by (41.5), is localized around the point $\xi = \lambda$. This means that

$$W_f(\lambda, b) = (f, w_{\lambda b}) = (\widehat{f}, \widehat{w}_{\lambda b})$$

contains information in both time and frequency around the point (b, λ).

For numerical computations, the coefficients $W_f(\lambda, b)$ are evaluated on a grid $(m\lambda_0, nb_0)$ with $m, n \in \mathbb{Z}$ and $\lambda_0, b_0 > 0$. One thus obtains a double sequence $W_{m,n}(f) = W_f(m\lambda_0, nb_0)$, which is a discretized version of the function of the two real variables λ and b.

41.4 Comparing the methods of Fourier and Gabor

The transforms of Fourier and Gabor, which we can write formally as

$$f(x) = \int_{-\infty}^{+\infty} \widehat{f}(\xi) e^{2i\pi x\xi} \, d\xi,$$

$$f(x) = \int_{\mathbb{R}^2} W_f(\lambda, b) w_{\lambda b}(x) \, d\lambda \, db,$$

can be interpreted as decomposing the signal f in terms of functions that play the role of basis functions, except that sums are replaced by integrals.

In the Fourier transform, these functions are sinusoids; in the Gabor transform, they are strongly attenuated sinusoids, or looked at the other way, modulated Gaussians (Figure 41.5). In the frequency space, we have the representations illustrated in Figure 41.6.

With Fourier's method, the "basis functions" are completely concentrated in frequency (Dirac impulses) and totally distributed in time (unattenuated sinusoids extending from $-\infty$ to $+\infty$). This is another way to explain that taking the Fourier transform gives the maximum amount of information about the distribution of the frequencies but completely loses information relative to time.

With Gabor's method, the figures show that time–frequency information remains coupled, although there is always a compromise: The uncertainty principle limits the simultaneous localization in time and frequency. In spite

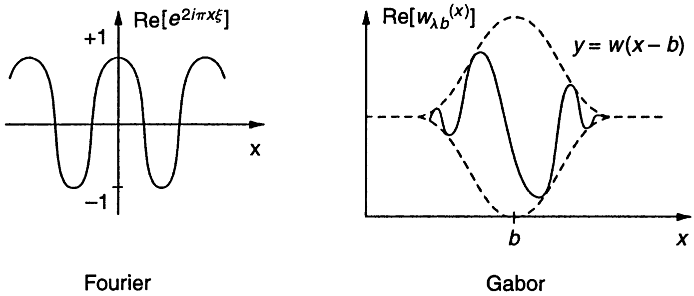

FIGURE 41.5. Basis functions for Fourier and Gabor decompositions.

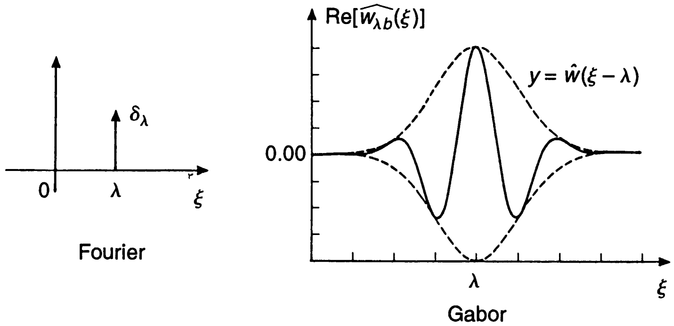

FIGURE 41.6. Basis functions for Fourier and Gabor in frequency space.

of this—which is a fact of life for any time–frequency analysis—Gabor's method has advantages over Fourier analysis for certain applications.

A signal f of finite duration provides one of the best illustrations of the difference between the two methods. The reconstruction of f using the inverse Fourier formula necessitates knowing the values of $\widehat{f}(\xi)$ with considerable precision over a very large range of values, for although $\widehat{f}(\xi)$ tends to zero, it can do so frustratingly slowly (consider the transform of $\chi_{[a,b]}$). The effects of all the sinusoids must come together to give zero outside the support of f.

The situation is quite different for Gabor analysis. It f vanishes on a long enough interval $(b_0 - \alpha, b_0 + \alpha)$ and if $w(t)$ is small for $|t| \geq 1$, then the coefficients $W_f(\lambda, b)$ will be negligible for b in a neighborhood of b_0, since

$$W_f(\lambda, b) \approx \int_{b-1}^{b+1} f(t)\overline{w}_{\lambda b}(t)\,dt = 0.$$

On the other hand, if f oscillates strongly at $t = b_0$, the value of $W_f(\lambda, b)$ will be large for b near b_0 when the values of λ "match" the frequency of f near b_0. This gives an idea about the "local frequency" of f.

In spite of its advantages for certain applications, the Gabor method has the major disadvantage that the size of the window is fixed. In terms of the uncertainty principle, this means that Δt is fixed (Section 22.3), and this limits the ability to localize events in time. Problems arise when one wishes to analyze signals that contain features on scales that range over several orders of magnitude. This is the case, for example, with speech. Consider the word "school." It begins with a short high-frequency attack followed by a longer relatively lower-frequency component. Fluid mechanics provides another important example. In fully developed turbulence, one observes events on scales that range from the macroscopic to the microscopic.

The geophysicist Jean Morlet encountered these kinds of problems in connection with seismic exploration for oil. Here it is necessary to analyze signals that result from a pulse being reflected (and delayed and compressed) from various layers in the earth. This led Morlet to introduce a new method where the window is not only translated but is also dilated and contracted. This was the beginning of the use of wavelets for numerical signal processing.

41.5 Exercises

Exercise 41.1 With the notation and hypotheses of Theorem 41.3.1, show that for f and $g \in L^2(\mathbb{R})$,

$$\iint_{\mathbb{R}^2} W_f(\lambda, b)\overline{W}_g(\lambda, b)\, d\lambda\, db = \int_{\mathbb{R}} f(t)\overline{g}(t)\, dt.$$

Exercise 41.2 Consider the signal $f(t) = e^{2i\pi\alpha t}$, $\alpha \in \mathbb{R}$, and the Gaussian window $w(t) = e^{-\pi t^2}$.

(a) Verify that

$$W_f(\lambda, b) = \int_{\mathbb{R}} f(t)\overline{w}(t-b)e^{-2i\pi\lambda t}\, dt$$

is well-defined (even though $f \notin L^2(\mathbb{R})$).

(b) Compute $W_f(\lambda, b)$ using the following result:

$$\text{For } a > 0 \text{ and } x \in \mathbb{R}, \quad \int_{\mathbb{R}} e^{-\pi a(t+ix)^2}\, dt = a^{-\frac{1}{2}}.$$

(c) Show that $|W_f(\lambda, b)|^2$ attains its maximum when $\lambda = \alpha$.

Exercise 41.3 Consider the Gaussian window $w(t) = Ae^{-\alpha t^2}$ with $A, \alpha > 0$ and the signal $f(t) = Be^{-\beta t^2}$ with $B, \beta > 0$. Use the result in Exercise 41.2(b) to compute

$$W_f(\lambda, b) = \int_{\mathbb{R}} f(t)\overline{w}(t-b)e^{-2i\pi\lambda t}\, dt.$$

Lesson 42

Wavelet Analysis

Gabor's method dates from the 1940s. With wavelets we enter a dynamic contemporary research environment; what is now known as the modern theory of wavelets emerged in the 1980s, notably with the article [GM84] by Alex Grossmann and Jean Morlet. We say "modern" wavelet theory because looking back over the mathematical landscape from a late twentieth century perspective we can identify many earlier ideas and techniques that are now logically included in this theory. Work by Haar in 1909; work in the late 1920s by Strömberg; results from the 1930s by Littlewood and Paley, Lusin, and Franklin; and later work in the 1960s, particularly the result of Calderón on operators with singular kernels—all these efforts and others are now interpreted in the language of wavelets.

What happened in the 1980s was qualitatively different; there occurred a conjunction of requirement and solution. Jean Morlet, a geophysicist, wished to analyze a particular class of signals associated with seismic exploration, and he had an idea about how this should be done. He sought the collaboration of Alex Grossmann, who, being a theoretical physicist, had command of certain mathematical tools, particularly those associated with coherent states and group representations from quantum theory. The immediate result was their celebrated 1984 paper; it was also the beginning of a productive collaboration between mathematics and other sectors of science and technology. We will say more about contemporary research at the end of the lesson, once some basic results have been established.

42.1 The basic idea: the accordion

Starting with a function ψ, called the analyzing wavelet or "mother" wavelet, we construct the family of functions

$$\psi_{ab}(t) = \frac{1}{\sqrt{a}}\psi\left(\frac{t-b}{a}\right), \quad b \in \mathbb{R},\ a > 0.$$

The wavelet coefficients of a signal f are the numbers

$$C_f(a,b) = (f, \psi_{a,b}) = \int_{-\infty}^{+\infty} f(t)\overline{\psi}_{a,b}(t)\, dt.$$

The properties of ψ are quite different from those of a window, which has more or less the aspect of a characteristic function, while ψ, on the other hand, oscillates and its integral is zero. We also want ψ and $\widehat{\psi}$ to be well localized, which means that they both converge to zero at infinity fairly rapidly. In this way one obtains a function that looks like a wave: It oscillates and quickly decays. This is the source of its name. Morlet used the function

$$\psi(t) = e^{-\frac{t^2}{2}} \cos 5t,$$

which is now known as Morlet's wavelet; derivatives of the Gaussian are widely used in practice. Figures 42.1–42.4 illustrate differences in the behavior of the Gabor functions $w_{\lambda b}(t)$, which have a ridged envelope, and wavelets, which are dilated and contracted. With wavelets one sees the action of an accordion. (The factor $a^{-1/2}$ has not been used in the figures.) Unlike Gabor functions, wavelets do not have a rigid envelope.

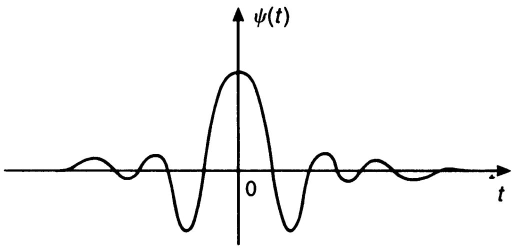

FIGURE 42.1. A wavelet oscillates and decays.

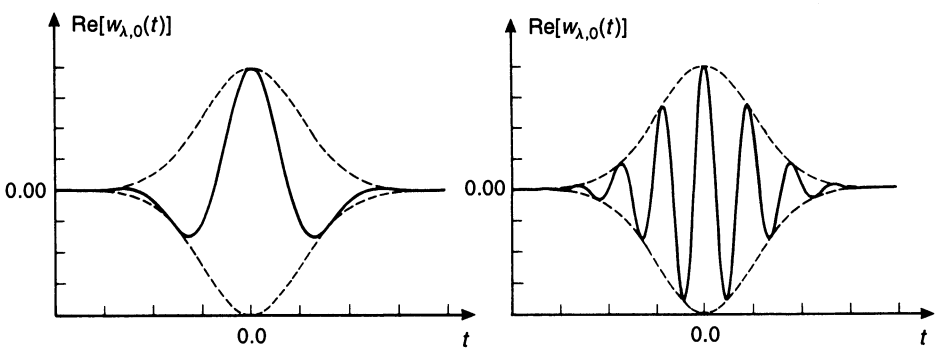

FIGURE 42.2. Gabor functions $w_{\lambda b}(t) = e^{-\frac{1}{2}(t-b)^2} e^{2i\pi\lambda t}$: The envelope is rigid, and the number of oscillations varies with frequency.

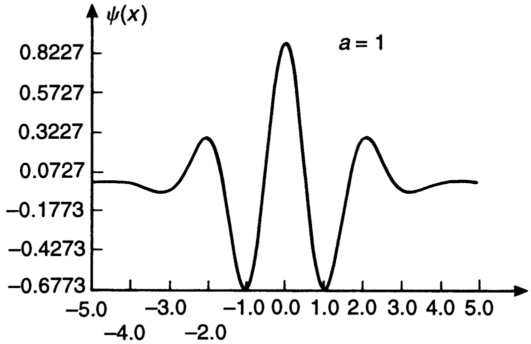

FIGURE 42.3. A mother wavelet (8th derivative of a Gaussian).

42.2 The wavelet transform

42.2.1 Theorem *Suppose that the function $\psi \in L^1(\mathbb{R}) \cap L^2(\mathbb{R})$ satisfies the following conditions:*

(i) $\displaystyle\int_{-\infty}^{+\infty} \frac{|\widehat{\psi}(\lambda)|^2}{|\lambda|}\, d\lambda = K < +\infty.$

(ii) $\|\psi\|_2 = 1.$

Construct the family of wavelets

$$\psi_{ab}(t) = \frac{1}{\sqrt{|a|}}\psi\left(\frac{t-b}{a}\right), \quad a, b \in \mathbb{R},\ a \neq 0,$$

and for any signal $f \in L^2(\mathbb{R})$ consider the wavelet coefficients

$$C_f(a,b) = \int_{-\infty}^{+\infty} f(t)\overline{\psi}_{ab}(t)\, dt.$$

Under these conditions we have the following results:

(a) *Conservation of energy:*

$$\frac{1}{K}\iint_{\mathbb{R}^2} |C_f(a,b)|^2 \frac{da\, db}{a^2} = \int_{-\infty}^{+\infty} |f(t)|^2\, dt.$$

(b) *Reconstruction formula:*

$$f(x) = \frac{1}{K}\iint_{\mathbb{R}^2} C_f(a,b)\psi_{ab}(x)\frac{da\, db}{a^2}$$

in the sense that if

$$f_\varepsilon(x) = \frac{1}{K}\iint_{\substack{|a|\geq\varepsilon \\ b\in\mathbb{R}}} C_f(a,b)\psi_{ab}(x)\frac{da\, db}{a^2},$$

then $f_\varepsilon \to f$ in $L^2(\mathbb{R})$ as $\varepsilon \to 0^+$.

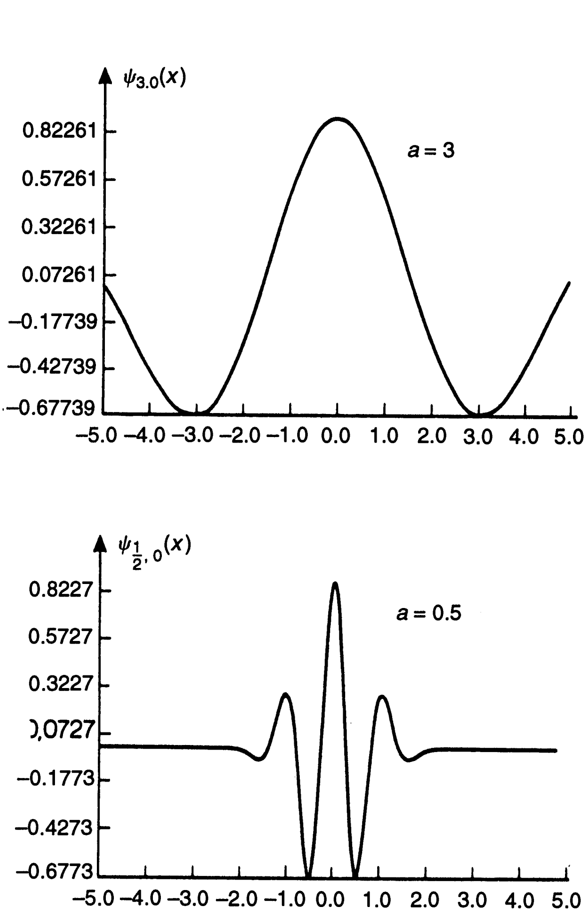

FIGURE 42.4. Wavelets at low and high frequency: They have the same form and the same number of oscillations; they are dilated for large a and contracted for small a.

Proof. First two observations: The ψ_{ab} are normalized so that $\|\psi_{ab}\|_2 = 1$, and the proof is similar to that of Theorem 41.3.1. Thus, as before, we find another expression for $C_f(a, b)$:

$$C_f(a,b) = \int_{-\infty}^{+\infty} f(t)\overline{\psi}_{ab}(t)\, dt = \int_{-\infty}^{+\infty} \widehat{f}(\lambda)\overline{\widehat{\psi}}_{ab}(\lambda)\, d\lambda,$$

and since

$$\widehat{\psi}_{ab}(\lambda) = \sqrt{|a|}e^{-2i\pi\lambda b}\widehat{\psi}(a\lambda), \tag{42.1}$$

we have

$$C_f(a,b) = \sqrt{|a|}\,\overline{\mathscr{F}}_{\lambda}\big[\widehat{f}(\lambda)\overline{\widehat{\psi}}(a\lambda)\big](b). \tag{42.2}$$